

Quantifying population dynamics via a geometric mean predator-prey model

Original

Quantifying population dynamics via a geometric mean predator-prey model / da Silva, S.L., Carbone, A., Kaniadakis, G.. - In: CHAOS. - ISSN 1054-1500. - 33:8(2023). [10.1063/5.0158723]

Availability:

This version is available at: 11583/2981549 since: 2023-09-04T07:33:48Z

Publisher:

American Institute of Physics

Published

DOI:10.1063/5.0158723

Terms of use:

This article is made available under terms and conditions as specified in the corresponding bibliographic description in the repository

Publisher copyright

(Article begins on next page)

RESEARCH ARTICLE | AUGUST 03 2023

Quantifying population dynamics via a geometric mean predator–prey model

S. L. da Silva   ; A. Carbone  ; G. Kaniadakis 



Chaos 33, 083102 (2023)

<https://doi.org/10.1063/5.0158723>



CrossMark

Articles You May Be Interested In

Bifurcations, chaos, and multistability in a nonautonomous predator–prey model with fear

Chaos (December 2021)

The food web prey-predator model with toxin

AIP Conference Proceedings (October 2020)

Diffusion-induced regular and chaotic patterns in a ratio-dependent predator–prey model with fear factor and prey refuge

Chaos (March 2021)

04 September 2023 08:11:14

AIP Advances

Why Publish With Us?

 25 DAYS average time to 1st decision	 740+ DOWNLOADS average per article	 INCLUSIVE scope
--	--	---

[Learn More](#)



Quantifying population dynamics via a geometric mean predator–prey model

Cite as: Chaos 33, 083102 (2023); doi: 10.1063/5.0158723

Submitted: 17 May 2023 · Accepted: 13 July 2023 ·

Published Online: 3 August 2023



View Online



Export Citation



CrossMark

S. L. da Silva,^{1,2,a} A. Carbone,¹ and G. Kaniadakis¹

AFFILIATIONS

¹Department of Applied Science and Technology, Politecnico di Torino, 10129 Turin, Italy

²GISIS, Fluminense Federal University, Campus Praia Vermelha, 24210-346 Niterói/RJ, Brazil

^aAuthor to whom correspondence should be addressed: sergio.dasilva@polito.it

ABSTRACT

An integrable Hamiltonian variant of the two species Lotka–Volterra (LV) predator–prey model, shortly referred to as *geometric mean (GM) predator–prey model*, has been recently introduced. Here, we perform a systematic comparison of the dynamics underlying the GM and LV models. Though the two models share several common features, the geometric mean dynamics exhibits a few peculiarities of interest. The structure of the scaled-population variables reduces to the simple harmonic oscillator with dimensionless natural time T_{GM} varying as $\omega_{GM} t$ with $\omega_{GM} = \sqrt{c_{12} c_{21}}$. We found that the natural timescales of the evolution dynamics are amplified in the GM model compared to the LV one. Since the GM dynamics is ruled by the inter-species rather than the intra-species coefficients, the proposed model might be of interest when the interactions among the species, rather than the individual demography, rule the evolution of the ecosystems.

© 2023 Author(s). All article content, except where otherwise noted, is licensed under a Creative Commons Attribution (CC BY) license (<http://creativecommons.org/licenses/by/4.0/>). <https://doi.org/10.1063/5.0158723>

Despite its extreme simplicity, the Lotka–Volterra (LV) predator–prey model does not admit a closed-form analytical solution, and for this reason, numerical integration methods are usually adopted to apply it to various fields of science. The present paper presents a model for describing a new predator–prey interaction called the geometric mean (GM) model. The GM model shares the broad features of the standard LV one and, at the same time, offers the advantage of possessing closed-form exact analytical solutions. The GM model allows the analysis of predator–prey dynamics through a Hamiltonian approach and may be described by the well-established physics of harmonic oscillators.

gaining importance in strategic planning and policy decision-making in relation to sustainability issues.

The LV two-species model is described by the coupled first-order differential equations:

$$\frac{dx_1}{dt} = c_{12} x_1 x_2 - c_{11} x_1, \quad (1a)$$

$$\frac{dx_2}{dt} = -c_{21} x_1 x_2 + c_{22} x_2, \quad (1b)$$

where $x_1(t)$ and $x_2(t)$ are positive functions representing predator and prey populations at time $t \geq 0$. The positive parameters c_{ij} characterize the predator–prey interaction ($i \neq j$) and the mortality–birth rate ($i = j$). In particular, c_{11} represents the predator’s mortality (migration) rate, while c_{22} is the prey’s birth rate. The terms $c_{12} x_1 x_2$ and $-c_{21} x_1 x_2$ stand for the growth rate of the predator population and the predation rate of the prey population, respectively. The number of free parameters in Eqs. (1a) and (1b) can be reduced by scaling the variables

$$X_1 = \frac{c_{21}}{c_{11}} x_1, \quad X_2 = \frac{c_{12}}{c_{11}} x_2, \quad (2a)$$

$$T = c_{11} t, \quad r = \frac{c_{22}}{c_{11}}. \quad (2b)$$

I. INTRODUCTION

The Lotka–Volterra (LV) predator–prey model, independently proposed in Refs. 1 and 2, and its several variants put forward afterward^{3,4} have been widely used and still represent a paradigm⁵ in the nonlinear statistical analysis of population dynamics, with applications transcending the field of ecology,^{6–17} as, for example, in plasma physics,¹⁸ machine learning,¹⁹ and astrophysics.²⁰ Population dynamics analysis based on the LV description is increasingly

Then, the two-species LV equations for the scaled populations X_1, X_2 become

$$\frac{dX_1}{dT} = X_1 X_2 - X_1, \quad (3a)$$

$$\frac{dX_2}{dT} = -X_1 X_2 + r X_2, \quad (3b)$$

with r being the only one free-parameter.

The scaled populations admit two equilibrium points at $dX_1/dT = dX_2/dT = 0$ and singularity at $(X_1, X_2) = (0, 0)$ and $(X_1, X_2) = (r, 1)$. In the $X_1 X_2$ phase plane, the trajectories are described by the conserved quantity

$$H(X_1, X_2) = X_1 - r \ln(X_1) + X_2 - \ln(X_2), \quad (4)$$

with the initial conditions $H_0 = H(X_{10}, X_{20})$ with $H > H_{\min} = H(r, 1) = 1 + r[1 - \ln(r)]$. The conserved quantity H depends on the parameter r and on the initial conditions X_{10} and X_{20} and plays the role of the Hamiltonian or Lyapunov function of the LV system.²¹ The bounds for the predator and prey populations follow directly by examining the trajectory $H(X_1, X_2) = H_0$,

$$-r W_+(a) \leq X_1 \leq -r W_-(a) \quad \text{and} \quad -W_+(b) \leq X_2 \leq -W_-(b), \quad (5)$$

where W_{\pm} are the principal and negative branches of the Lambert function, with $a = -r^{-1} e^{(1-H_0)/r}$ and $b = -r^{-r} e^{r-H_0}$. Despite the deep insight gained through the LV model and its successful applications, a number of drawbacks are still outstanding, which prevent a thorough comprehension of the dynamics underlying real-world system evolution.^{18,22} The standard LV model is not integrable and, thus, is mainly studied numerically. Its solution is notoriously periodic³ with the exact expression of the oscillation frequency unknown, except in its linearized version.

A Hamiltonian predator–prey model, shortly referred to as *geometric mean (GM) predator–prey model*, capturing the main features of the standard LV model and admitting exact solutions in terms of elementary functions has been recently proposed.²³ In the GM model, the growth and death rates are proportional to the square root of the populations $\sqrt{x_i}$ rather than the populations themselves x_i . Similar behavior is also assumed for the predating rate on prey whose food supply depends on the square root of the prey population. The interaction between predator and prey populations is described by the geometric mean of the two populations $\sqrt{x_1 x_2}$, implying that the growth rate of the predator population are $c_{12} \sqrt{x_1 x_2}$ and $-c_{21} \sqrt{x_1 x_2}$, respectively.

This work is aimed at comparing the geometrical mean model to the standard Lotka–Volterra model by numerically solving the differential equations and highlighting similarities and differences in the underlying dynamics. In particular, we show that the evolution dynamics' timescale of the LV model is amplified in the GM model, which is driven by the inter-species rather than the intra-species interactions. Hence, while the characteristic time of the LV dynamics simply depends on the predator mortality, the characteristic time of the GM model depends on the joint effect of the growth rate of the predator population and the death rate of the prey population. The difference is summarized in r , the only parameter which appears in the rescaled GM and LV models. While in

the latter r depends only on the demographic parameters, in the GM model, r depends also on the interaction strength between the populations. These results open new scenarios in the modeling of population dynamics to analytically describe the predator–prey time evolution when the dynamics is driven by the interaction between the two species rather than by the demographic features of each species. As stated above, the main purpose of this work is to highlight the structural differences in the mean field description of the two models hence the current analysis is kept limited to the deterministic forms of the prey–predator dynamic equations. However, one should bear in mind that real-world ecosystems are featured by stochastic rather than deterministic interactions as already suggested in the early literature dealing with oscillatory phenomena in ecological and biological networks^{24,25} and still under active scrutiny. Additive and multiplicative noise sources affecting the interaction processes have been considered in Refs. 26–29, and 30. The onset of the oscillatory behavior and its offset have been related to the fluctuating interactions about the network entries accounted for in the framework of random matrix approaches.^{31–36} The eigenvalue spectrum between arbitrary pairs of the random matrix elements is investigated to ascertain the situations when off diagonal or circular other than diagonal elements might impact the system stability. Overall, the effects of fluctuations, in particular, those related to the inter-species terms (off diagonal entries of the random matrices) are highly relevant to the aging and extinction of a large class of interacting systems. Hence, though not included in the present discussion, one could expect that fluctuations emerging from asymmetric terms might play an important role in the geometric mean model where the inter-species dominate over the intra-species interactions.

The paper is organized as follows. In Sec. II, the main equations describing the geometric mean (GM) predator–prey dynamics model and its scaled form are briefly recalled. In Sec. III, we perform a comparative analysis from a computational viewpoint and discuss the outcomes of the analytical solutions against numerical ones. Then, we compare the two dynamics by analyzing the respective Hamiltonians. In Sec. IV, a few remarks on the outcomes and implications of the novel predator–prey model beyond current work are addressed.

II. GEOMETRIC MEAN PREDATOR–PREY MODEL (GM MODEL)

The geometric mean (GM) predator–prey model is described by the following coupled first-order differential equations:

$$\frac{dx_1}{dt} = c_{12} \sqrt{x_1 x_2} - c_{11} \sqrt{x_1}, \quad (6a)$$

$$\frac{dx_2}{dt} = -c_{21} \sqrt{x_1 x_2} + c_{22} \sqrt{x_2}, \quad (6b)$$

with $x_1 = x_1(t)$ and $x_2 = x_2(t)$ being the predator and the prey populations, as in the standard LV model.^{23,37} The positive parameters c_{11} and c_{22} characterize the mortality–birth rates. In particular, c_{11} represents the predator's mortality (migration) rate and reflects how fast the predator population declines in the absence of prey. It indicates the predators' natural mortality rate due to several aspects, such as diseases, aging, and resource competition among predators.

The parameter c_{22} represents the prey’s birth rate and reflects how quickly the prey population can grow in the absence of predators around. It indicates the prey population growth rate due to, for instance, the reproduction rate and resource availability. The positive parameters c_{12} and c_{21} represent the predator–prey interaction. In this regard, c_{12} describes the efficiency of the converting consumed prey into predator offspring and indicates the proportion of “prey energy” successfully transferred to the predator population, considering energy transfer aspects after a possible predator–prey binary interaction. Finally, c_{21} defines the predation rate and indicates how often the predators capture and consume the prey. The set of free parameters is reduced by scaling the variables according to

$$X_1 = \frac{c_{12} c_{21}}{c_{11}^2} x_1, \quad X_2 = \frac{c_{12}^2}{c_{11}^2} x_2, \quad (7a)$$

$$T = \sqrt{c_{12} c_{21}} t, \quad r = \frac{c_{22}}{c_{11}} \sqrt{\frac{c_{12}}{c_{21}}}. \quad (7b)$$

The scaled version of the equations reads

$$\frac{dX_1}{dT} = \sqrt{X_1 X_2} - \sqrt{X_1}, \quad (8a)$$

$$\frac{dX_2}{dT} = -\sqrt{X_1 X_2} + r\sqrt{X_2}. \quad (8b)$$

The geometric mean (GM) and the standard (LV) predator–prey model share the following features: (i) the appetite of predators is insatiable; (ii) food is always available in abundance to the prey community; (iii) the number of preys is the only source of food for the predator population’s; (iv) genetic variants and adaptations to habitat have little impact on predation dynamics since the environment conditions does not change in a way that benefits one over the other species.

The scaled GM populations admit two equilibrium points at $dX_1/dT = dX_2/dT = 0$, which are given by $(X_1, X_2) = (0, 0)$ and $(X_1, X_2) = (r^2, 1)$. The Hamiltonian of the system

$$H(X_1, X_2) = X_1 - 2r\sqrt{X_1} + X_2 - 2\sqrt{X_2} \quad (9)$$

is a conserved quantity whose value can be obtained from the initial conditions $H_0 = H(X_{10}, X_{20})$,

$$H_0 = \left(\sqrt{X_{10}} - r\right)^2 + \left(\sqrt{X_{20}} - 1\right)^2 - 1 - r^2, \quad (10)$$

which yields the minimum value of the Hamiltonian

$$H_{\min} = -1 - r^2, \quad (11)$$

for $X_{10} = r^2$ and $X_{20} = 1$. The trajectory of the system in the phase space is defined through $H(X_1, X_2) = H_0$. The latter relationship provides the bounds of X_1 and X_2

$$(r - c)^2 \leq X_1 \leq (r + c)^2 \quad \text{and} \quad (1 - c)^2 \leq X_2 \leq (1 + c)^2, \quad (12)$$

with $c = \sqrt{1 + H_0 + r^2}$.

The quadratic transformation

$$X_i = \frac{1}{4} Y_i^2 \quad (13)$$

provides the Hamiltonian counterpart for the canonical system in the following form:

$$\mathcal{H}(Y_1, Y_2) = \frac{1}{4} Y_1^2 - r Y_1 + \frac{1}{4} Y_2^2 - Y_2, \quad (14)$$

representing, in the phase space, the circle

$$(Y_1 - Y_{1c})^2 + (Y_2 - Y_{2c})^2 = R^2, \quad (15)$$

with $Y_{1c} = 2r$, $Y_{2c} = 2$, and $R^2 = (Y_{10} - Y_{1c})^2 + (Y_{20} - Y_{2c})^2$. The maximum and minimum values of the parameter r can be obtained by the conditions $Y_{1c} > R$ and $Y_{2c} > R$, i.e.,

$$\frac{X_{10} + (\sqrt{X_{20}} - 1)^2}{2\sqrt{X_{10}}} \leq r \leq \sqrt{X_{10}} + \sqrt{2\sqrt{X_{20}} - X_{20}}. \quad (16)$$

The Hamilton–Jacobi equations for the canonical system

$$\frac{dY_1}{dT} = \frac{\partial \mathcal{H}}{\partial Y_2}, \quad (17a)$$

$$\frac{dY_2}{dT} = -\frac{\partial \mathcal{H}}{\partial Y_1} \quad (17b)$$

allow writing the evolution equations for the canonical populations $Y_i = 2\sqrt{X_i}$ in the following form:

$$\frac{dY_1}{dT} = \frac{1}{2} Y_2 - 1, \quad (18a)$$

$$\frac{dY_2}{dT} = r - \frac{1}{2} Y_1. \quad (18b)$$

The system of linear Eqs. (18a) and (18b) can be easily decoupled, resulting in a simple harmonic oscillator-type model as follows:

$$\frac{d^2 Y_i}{dT^2} + \frac{1}{4} Y_i = \frac{1}{2} r^{2-i}, \quad (19)$$

for $i = 1, 2$. In this regard, note that the GM model enables the use of a general and well-established physics of harmonic oscillators to model the dynamics of prey–predator dynamics. The solution of Eq. (19) is remarkable and, by using Eq. (13), the scaled populations X_i write

$$X_1(T) = \left[r + \left(\sqrt{X_{10}} - r\right) \cos(\omega T) + \left(\sqrt{X_{20}} - 1\right) \sin(\omega T) \right]^2, \quad (20a)$$

$$X_2(T) = \left[1 + \left(\sqrt{X_{20}} - 1\right) \cos(\omega T) - \left(\sqrt{X_{10}} - r\right) \sin(\omega T) \right]^2, \quad (20b)$$

where $\omega = 1/2$ is the angular frequency. The populations $x_i(t)$ can be obtained from the scaled populations $X_i(T)$, Eqs. (20a) and (20b), by using Eqs. (7a) and (7b).

The functions $X_1(T)$ and $X_2(T)$ in Eqs. (20a) and (20b) are the analytical solutions of the GM model.²³ In Sec. III, the behavior of

the geometric mean predator–prey model to the standard LV will be compared. As the LV model does not admit an analytical solution, various computational steps are required for numerically evaluate the related differential equations. These issues will be addressed in Sec. III.

III. COMPARISON OF THE GEOMETRIC MEAN (GM) AND LOTKA-VOLTERRA (LV) PREDATOR-PREY DYNAMICS

The first step to numerically solve the LV differential equation system is concerned with the choice of the numerical method to be adopted among the several available approaches. We consider seven different numerical methods for the solution of ordinary differential equation (ODE) well established in the literature.³⁸ The methods are labeled by the acronyms: ODE-15-S, ODE-23, ODE-23-S, ODE-23-T, ODE-23-TB, ODE-45, and ODE-113. In the acronyms, the figures refer to the order of accuracy of the numerical integration scheme, while capital letters refer to performed upgrades in these schemes. The ODE-15-S method is a variable-order (from first to fifth) numerical solver widely employed for solving differential-algebraic equations and stiff ODEs.³⁹ The ODE-23 is a low-order integration method commonly used to solve nonstiff ODEs based on the second- and third-order Runge–Kutta (RK) technique, also known as the Bogacki–Shampine scheme. The ODE-23-S is an alternative to the classical ODE-23 approach, which is used in solving stiff ODEs based on a modified Rosenbrock triple scheme related to implicit RK methods.³⁹ The ODE-23-T and ODE-23-TB integration methods are widely employed to solve stiff ODEs based on an implicit RK formula using the trapezoidal rule for approximating numerical computing of a definite integral. In the ODE-23-TB case, the numerical calculation of the definite integral is carried out with a second-order backward differentiation formula.³⁹ The ODE-45 is a medium-order integration method widely employed to solve nonstiff ODEs based on the fourth and fifth-order RK method, also known as the Dormand–Prince scheme. Finally, the last one is a high-precision solver for solving nonstiff differential equations,³⁹ namely, the ODE-113.

To address the accuracy issues with the above integration schemes in solving the GM model evolution Eqs. (8a) and (8b), we consider 5000 time samples with $T \in [0, 30]$, $r = 1.2$ and $X_{10} = X_{20} = 2$. Then, we compare the obtained numerical solutions with the analytical ones given by Eqs. (20a) and (20b). To quantify the accuracy of each numerical result, we use the normalized root mean square (NRMS) defined through $NRMS = \sqrt{\sum_i (x_i^{true} - x_i^{nsol})^2 / \sum_i (x_i^{true})^2}$, where x_i^{true} and x_i^{nsol} are the exact analytical and numerical solutions, respectively. The range of NRMS values varies from 0 (minimum error) to ∞ (maximum error). The NRMS and the runtime for the numerical simulations are summarized in Table I. We notice that no numerical method perfectly solves the system of ODE under analysis. In addition, the fastest method (ODE-23-TB) performs with a runtime 51.40 slower compared to the analytical solution. The most accurate numerical integration method (ODE-113) solves the novel predator–prey equations with a runtime 138.44 times slower than the exact analytical solution. The numerical experiments confirm that solving

TABLE I. The normalized root mean square (NRMS) and the runtime for the numerical simulations using the novel scaled predator–prey model.

Numerical method	Runtime 1 runtime = 2.5 ms	NRMS	
		$X_1(T)$	$X_2(T)$
Analytical solution	1.00	0.0000	0.0000
ODE-23-TB	51.40	0.0070	0.0069
ODE-23-S	54.41	0.0068	0.0059
ODE-23	65.91	0.0024	0.0026
ODE-23-T	67.54	0.0076	0.0074
ODE-45	89.20	0.0039	0.0042
ODE-15-S	132.18	0.0032	0.0031
ODE-113	138.44	0.0005	0.0005

ODEs is time-consuming, making it difficult to use them to deal with real issues such as, for instance, modern big data analysis problems. Thus, simulating population dynamics by solving ODEs entirely depends on a good trade-off between runtime and tolerated numerical errors. These problems do not exist when the analytical solution is known.

In this section, we discuss the similarities and differences between the dynamics of the standard LV and the GM models. It is worth remembering that both dynamics follow a population growth and decline cycle of predators and prey, as discussed in Sec. II.^{***} However, the standard LV population model is exponential, while the GM model’s growth rate is quadratic. We simply eliminate the iteration term between the two species to analyze these rates. In this regard, from Eqs. (3a) and (3b), note that $\frac{dX_1}{dT} \propto X_1$ and $\frac{dX_2}{dT} \propto rX_2$ give the growth rates associated with the standard model, leading to $X_1(T) = X_{10} \exp(\alpha_1 T)$ and $X_2(T) = X_{20} \exp(r\alpha_2 T)$, where α denotes the proportionality and α_1 and α_2 proportionality constants. At the same time, from Eqs. (8a) and (8b), we notice that $\frac{dX_1}{dT} \propto \sqrt{X_1}$ and $\frac{dX_2}{dT} \propto r\sqrt{X_2}$ give the growth rates associated with the novel predator–prey model, leading to $X_1(T) = (\frac{1}{2}\alpha_1 T + \sqrt{X_{10}})^2$ and $X_2(T) = (\frac{r}{2}\alpha_2 T + \sqrt{X_{20}})^2$ for $X_{10}, X_{20} > 0$. A significant difference between the models is the impact of the predator–prey pair on each other. To interpret the behavior of the predation rate, we consider only the first terms of the two predator–prey models, i.e., $\frac{dX_1}{dT} = (X_1 X_2)^\alpha$ and $\frac{dX_2}{dT} = -(X_1 X_2)^\alpha$, in which the cases $\alpha = 1$ and $\alpha = 1/2$ represent the predator–prey interaction term related to the standard LV and GM models, respectively. In this regime, a monotonically growing population of predators is expected while the prey population decreases until extinction. Such a regime is described so that the scaled predator populations are given by $X_1(T) = X_0 - X_2(T)$, with $X_0 = X_{10} + X_{20}$, in both cases, while the scaled prey populations are, respectively, $X_2(T) = X_0/[1 - (1 - X_0/X_{20}) \exp(X_0 T)]$ for $T \in [0, \infty)$ and $X_2(T) = X_0 \sin^2(-\omega T + \arcsin(\sqrt{X_{20}/X_0}))$ for $T \in [0, T_{max}]$ in standard and new dynamics, where $T_{max} = 2 \arcsin(\sqrt{X_{20}/X_0})$. The standard LV model predicts infinite dynamics over time, even after prey extinction, i.e., $X_2(T \rightarrow \infty) = 0$. On the other hand, predators grow following a logistic curve $X_1(T) = X_0/(1 + (X_0/X_{20} - 1) \exp(-X_0 T))$, in which their population remains constant after a lack of food

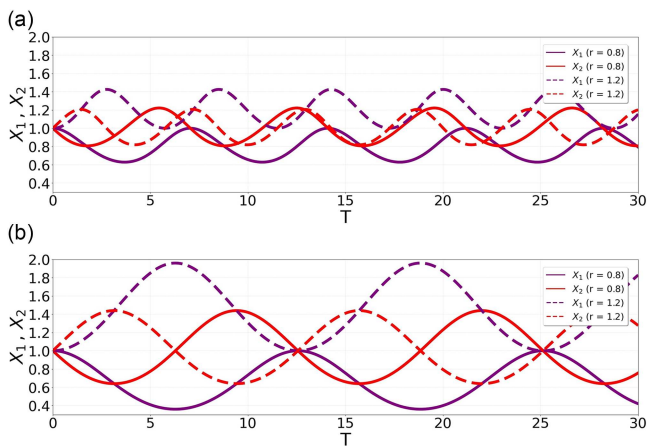


FIG. 1. Scaled predator (purple lines) and prey (red lines) populations as a function of the scaled time with initial conditions $X_{10} = X_{20} = 1.0$, and $r = 0.8$ (solid lines) and $r = 1.2$ (dashed lines), for (a) the standard LV model, and (b) the geometric mean (GM) model.

(prey extinction), i.e., $X_1(T \rightarrow \infty) = X_0$. In contrast, the GM model predicts a cessation in predation dynamics when the prey population is extinct at time T_{max} . As a result of the resistance of the environment, represented in this instance by the absence of prey, the GM model suggests the extinction of predation dynamics when $X_2(T_{max}) = 0$ and $X_1(T_{max}) = X_0$.

Figure 1 shows the time evolution of the scaled predator X_1 (purple) and prey X_2 (red) populations as a function of the scaled time T under the same initial conditions ($X_{10} = 1.0$ and $X_{20} = 1.0$) for the LV and the GM model. Solid curves refer to $r = 0.8$, while dashed lines refer to $r = 1.2$. A small change in the r -value from 0.8 to 1.2 noticeably affect the predator–prey dynamics. Since the oscillation frequency of the standard LV system is unknown, its dynamics may be explored by evaluating a Jacobian matrix⁴⁰ in an equilibrium point (that is, through a linearization process using first-order partial derivatives). When the standard LV model is

TABLE II. Pearson correlation coefficient (ρ) between the solutions of the LV and GM models, as depicted by the black and colored curves depicted in Fig. 2.

		$r_{GM} = r_{LV}$	$r_{GM} = 1.1 r_{LV}$	$r_{GM} = 0.9 r_{LV}$
X_1	$r_{LV} = 0.8$	−0.0256	−0.0283	−0.0224
	$r_{LV} = 1.2$	+0.0493	+0.0439	+0.0559
X_2	$r_{LV} = 0.8$	−0.0524	−0.0389	−0.0659
	$r_{LV} = 1.2$	−0.0117	−0.0347	+0.0114

scaled according to Eqs. (2a) and (2b), the oscillation frequency, in first-order approximation, around the equilibrium point ensues $\omega_{LV} = \sqrt{c_{22}/c_{11}}$. At the same time, the oscillation frequency associated with the GM model in its scaled version is constant with a period of 4π , as expected due to the factor $\omega = 1/2$ in the arguments of the sines and cosines functions in Eqs. (20a) and (20b). Such contrasts are noteworthy when we compare the predator–prey dynamics of the two models for different r -values for the GM model, as depicted in Fig. 2.

To quantitatively compare the fluctuations in population sizes shown in Fig. 2, we consider the Pearson correlation coefficient (ρ) as a similarity metric. In this regard, the Pearson coefficient statistically measures the degree of the linear relationship between two time series to assess the similarity between their fluctuations over time. This parameter ranges from -1 to 1 , in which a value close to 1 indicates a systematic association between changes in the fluctuations of the two signals, i.e., a strong positive correlation. On the other hand, a value close to -1 indicates that the amplitudes of the fluctuations tend to vary in opposite directions, i.e., a strong negative correlation. A value close to 0 indicates the absence of a systematic relationship between the fluctuations of the two signals, i.e., a weak correlation (or null when $\rho = 0$). We summarize in Table II the ρ -values between the colored and black curves depicted in Fig. 2. In all cases, Pearson coefficients assume values close to zero, indicating that the predator–prey models predict different fluctuations between them.

Figure 3 reports the predator–prey trajectories with initial conditions $X_{10} = 1.0$ and $X_{20} = 1.0$, and $r = 0.8$ (orange) and $r = 1.2$

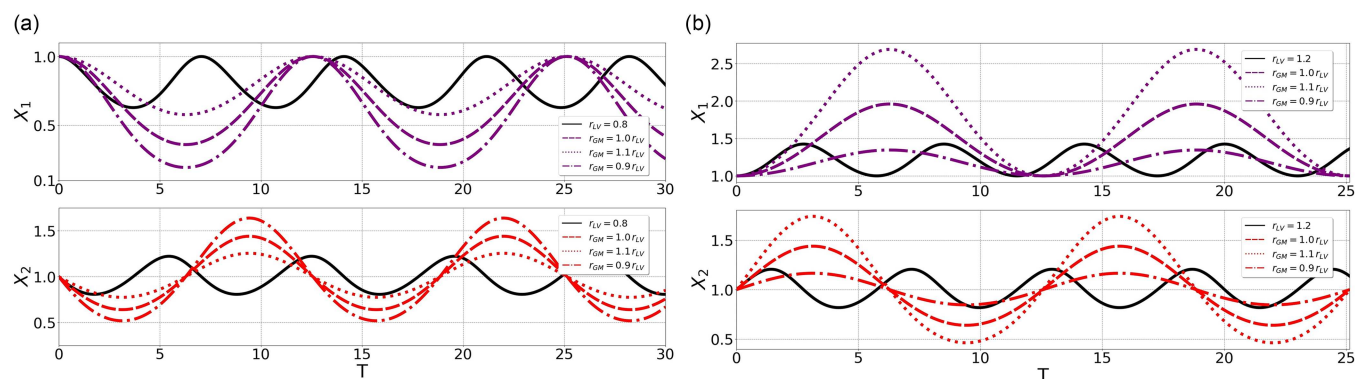


FIG. 2. Scaled predator and prey populations as a function of the scaled time with initial conditions $X_{10} = X_{20} = 1.0$, where the black curves refer to the Lotka–Volterra (LV) model with (a) $r = r_{LV} = 0.8$ and (b) $r = r_{LV} = 1.2$, while the colored curves refer to the geometric mean (GM) model.

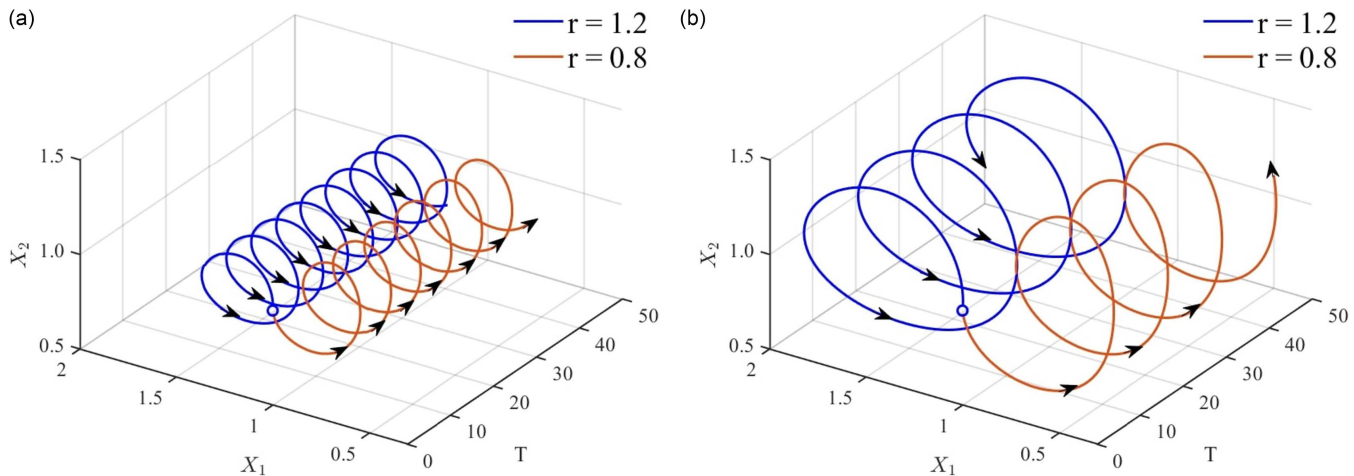


FIG. 3. The predator–prey trajectories with initial conditions $X_{10} = X_{20} = 1.0$, and $r = 0.8$ (orange lines) and $r = 1.2$ (blue lines), for (a) the standard LV model, and (b) the geometric mean (GM) model. The black arrows point to the direction of population variation along the increasing scaled-time T .

(blue), for (a) the standard LV model described by Eqs. (3a) and (3b) and (b) the GM model described by Eqs. (8a) and (8b). The black arrows point to the direction of the increasing scaled time. It is remarkable that the frequency of the evolution cycles is different for the two models. While in the standard LV model the frequency is a function of the parameter r , in the GM model, it is a constant $\omega = 1/2$. By considering $X_{10} = 1$ and $X_{20} = 1$, we notice that the GM model predicts a time evolution with population sizes more prominent than those predicted by the LV model for $r > 1$ (represented in Fig. 3 by the case $r = 1.2$; depicted by the blue lines) and smaller when $r < 1$ (represented in Fig. 3 by the case $r = 0.8$; depicted by the orange lines). This feature is because the r -parameter governs the insertion of energy, associated with environmental aspects that promote prey population growth, into the predator–prey scaled system. Indeed, as the prey and predator populations initiate to interact, their populations increase when $r > 1$, since the prey scaled-population variation rate (dX_2/dT) is positive, which induces an increase in the first term of Eqs. (3a) and (8b), leaving it to be more significant than the second term of these equations, conducting to the positivity of the predator scaled-population variation rate (dX_1/dT). When $r < 1$, the prey scaled-population variation rate, at the commencement of the dynamics, is less than zero, causing a decline of the prey population, which in turn induces the negativity of the predator scaled-population variation rate; therefore, both populations decrease in this regime at the beginning of the predator–prey iteration, as depicted by the orange lines in Fig. 3.

Figure 4 presents the phase portrait of the two models to assess the effect of the initial conditions on the predator–predator dynamics. The colored lines represent the phase plane trajectories corresponding to $r = 1.2$ and different values of the Hamiltonian (a) Eq. (4) for the standard LV model and (b) Eq. (9) for the GM model. The black dot represents the value of the predator and prey populations whose minimum Hamilton value is reached, i.e., when $(X_1 = r, X_2 = 1)$ and $(X_1 = r^2, X_2 = 1)$ in the LV model and in

the GM model, respectively. In both dynamics, the phase portraits exhibit closed trajectories that represent the possible population dynamics of predator and prey species. Although common patterns are observed, note that the minimum energy points (black dot in Fig. 4) are positioned differently along the X_1 -axis; they can be obtained in the steady state from Eqs. (3) and (8) for the LV and GM models, respectively. Such equilibrium points occur when $X_2 = 1$ in both dynamics, but it ensues for different values of X_1 , being $X_1 = r$ in the LV case and $X_1 = r^2$ in the GM case. The existence of this equilibrium point suggests that if both populations are extinct, they will remain extinct until an outside factor can change that.⁴ Also, predator and prey populations’ maximum and minimum possible values differ in both dynamics following Eq. (5) for the LV model and Eq. (12) for the GM dynamics.

Figure 5 reports the phase plane trajectories related to constant values of Hamiltonian with initial conditions $X_{10} = 2.0$ and $X_{20} = 1.5$, for some different r -values. The panel (a) refers to the standard LV model, while panel (b) refers to the GM model. It is remarkable that the minimum and maximum populations of predators (i.e., $X_{1\min}$ and $X_{1\max}$) are increasing functions of the parameter r in the two models. For the prey population, the behavior of $X_{2\min}$ and $X_{2\max}$ can be an increasing or decreasing function depending on the r -value. In both dynamics, $X_{2\min}$ is an increasing function of the r -parameter for $r < X_{10}$ in the case of the LV model and $r < \sqrt{X_{10}}$ in the GM model. At the same time, $X_{2\min}$ is a decreasing function of the r -parameter for $r > X_{10}$ in the case of the LV model and $r > \sqrt{X_{10}}$ in the GM model. We notice a similar behavior for the maximum value of the prey population, where $X_{2\max}$ decreases with r when $r < \sqrt{X_{10}}$ in the GM model case ($r < X_{10}$ in the LV dynamics), while $X_{2\max}$ becomes an increasing function when $r > \sqrt{X_{10}}$ in the GM model ($r > X_{10}$ in the LV dynamics). The orbit with $r = \sqrt{X_{10}}$ for the GM model and the one with $r = X_{10}$ for the LV model are depicted by black lines in Fig. 5. We notice the existence of two nodes in both dynamics, equally positioned along the X_1 -axis.

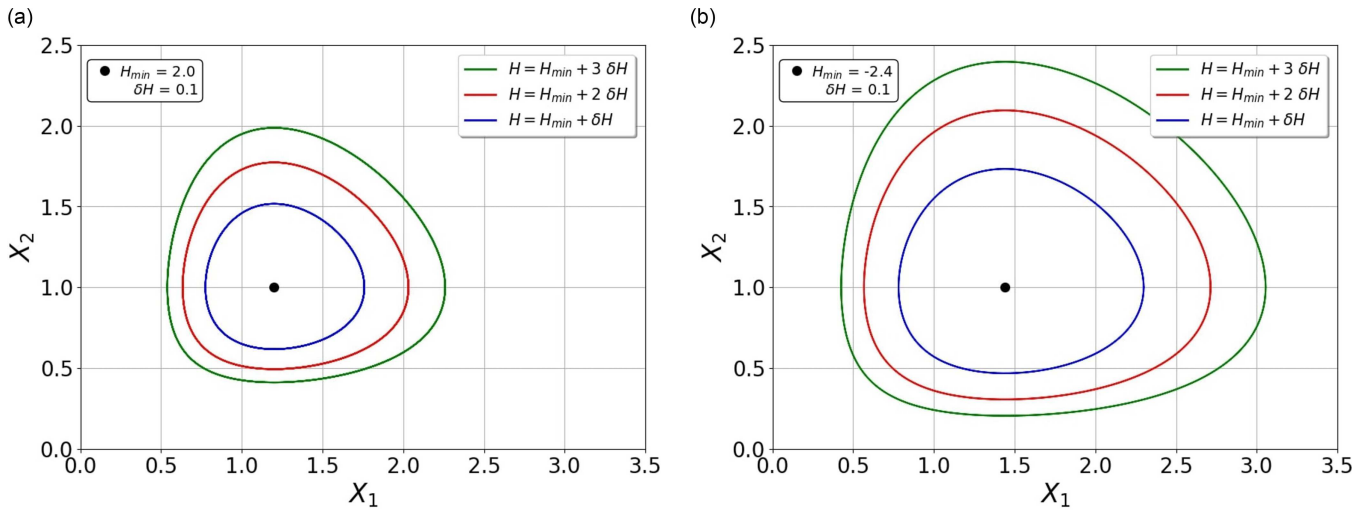


FIG. 4. Phase plane trajectories for three different values of the Hamiltonian, with $r = 1.2$, for (a) the standard LV model where $H_{\min} = 1 + r[1 - \ln(r)]$, and (b) the geometric mean (GM) model where $H_{\min} = -1 - r^2$.

In this case, the maximum $X_{2\max} = X_{20}$ and minimum $X_{2\min} = X_2^*$ values of the prey population are reached when $X_1 = X_{10}$ and defines two nodes (X_{10}, X_{20}) , (X_{10}, X_2^*) as shown in Fig. 5. The upper node corresponds to the starting point (X_{10}, X_{20}) at $T = 0$. The employed time T to reaches the lower node (X_{10}, X_2^*) is an increasing function of the r -parameter for both models. The two nodes can be obtained from the conservation of the Hamiltonian by solving the algebraic system

$$H(X_1, X_2, r_1) = H(X_{10}, X_{20}, r_1), \tag{21a}$$

$$H(X_1, X_2, r_2) = H(X_{10}, X_{20}, r_2), \tag{21b}$$

involving two different r -parameters. For the standard LV model, $X_2^* = -W_+(s)$ for $X_{20} > 1$ and $X_2^* = -W_-(s)$ for $X_{20} < 1$, where $s = -X_{20} e^{-X_{20}}$. For the GM model, the mathematical expression of

X_2^* is much more straightforward without needing the use of special functions and is given by the expression $X_2^* = (2 - \sqrt{X_{20}})^2$.

Figure 6 illustrates the orbits, when the r -parameter ranges from 0.6 to 1.5, in the phase space for the two models [panel (a) for the LV model and (b) for the GM model] in the special case where the two nodes collapse in a unique one, i.e., $(X_{10}, X_2^* = X_{20})$. This node is given by $(X_{10} = r, X_{20} = 1)$ and $(X_{10} = r^2, X_{20} = 1)$, for the LV and the GM model, respectively. For the orbits on the right-hand side of the node, corresponding to $r > \sqrt{X_{10}}$ for the GM model and $r > X_{10}$ for the LV model, the maximum predator $X_{1\max}$ and prey $X_{2\max}$ populations are increasing functions of the r -parameter in both the models. The minimum prey population $X_{2\min}$ is a decreasing function of the r -parameter, while the minimum predator population does not vary with the r -parameter and assumes the value $X_{1\min} = X_{10}$. For the orbits on the left-hand

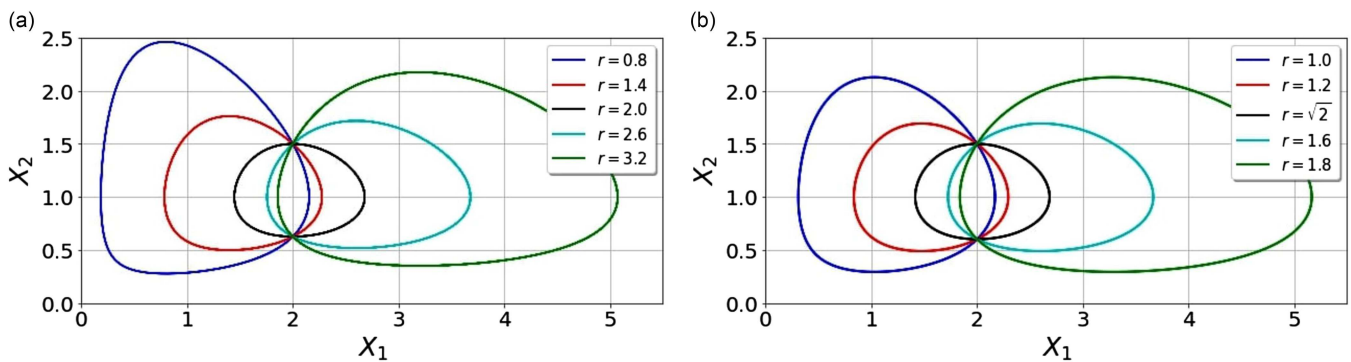


FIG. 5. Phase plane trajectories related to constant values of Hamiltonian with initial conditions $X_{10} = 2.0$ and $X_{20} = 1.5$, for some different r -values. The panel refers to (a) the standard LV model, while panel (b) refers to the geometric mean (GM) model. The upper node corresponds to the starting point (X_{10}, X_{20}) at $T = 0$. The employed time T to reaches the lower node (X_{10}, X_2^*) is an increasing function of the r -parameter.

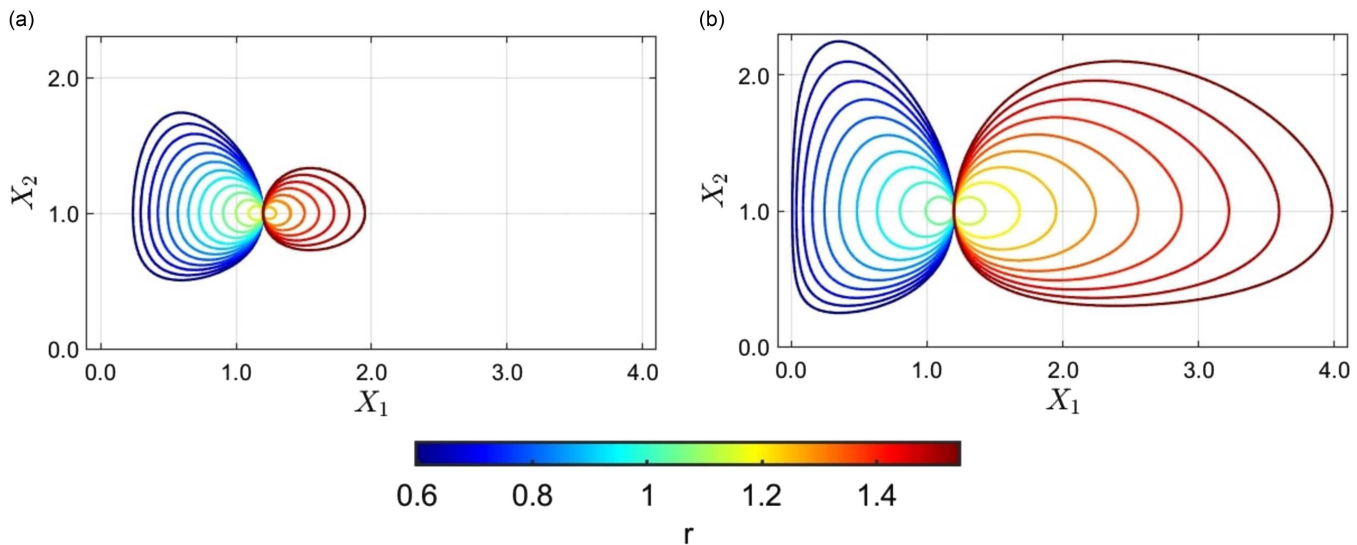


FIG. 6. Phase portraits for various r -values, ranging from 0.6 to 1.5, with $X_{10} = 1.2$ and $X_{20} = 1.0$ for (a) the standard LV model and (b) the geometric mean (GM) model.²³ The periodic orbits have a fixed energy at H_0 and are around the fixed node at the point $(X_{10}, 1)$.

side of the node, corresponding to $r < \sqrt{X_{10}}$ for the GM model and $r < X_{10}$ for the LV model, the maximum predator population remains fixed at the value $X_{1\max} = X_{10}$, while the maximum prey population $X_{2\max}$ is a decreasing function of the r -parameter. The minimum predator $X_{1\min}$ and prey $X_{2\min}$ populations are increasing functions of the r -parameter. Although the GM model predicts a dynamic with larger predator-prey populations than the LV one for the same r -value (prey *per capita* growth rate), both exhibit stable limits in the phase portrait even when the initial conditions coincide with the equilibrium point ($X_2 = 1$ in both models, $X_1 = r$ and $X_1 = r^2$ for the LV and GM models, respectively), except for the case $r = 1$.

Figure 7 shows the contour plot under surface basemap representing the two models' Hamiltonian from a three-dimensional perspective for $r = 0.5$, $r = 1.0$, and $r = 1.5$. The left column refers to the standard LV model, while the right one refers to the novel predator-prey model. The region annotated with colors closest to dark red (representative of the smallest amplitudes among the H-values) is centered on the equilibrium point $(r, 1)$ for the standard LV model and $(r^2, 1)$ for the GM model. From a visual inspection, the similarities between the Hamiltonians are noticeable, although they have different mathematical expressions. When $r = 0.5$, it is worth noting that both population models predict rapid predator growth [Figs. 7(a) and 7(b)], while in the case of $r = 1.5$, the prey population's growth is drastically impacted, as depicted in Figs. 7(e) and 7(f). In other words, the r -parameter directly influences which species dominate the energy content of the predator-prey dynamics. When r takes on the value of 1, the 3D representation of the Hamiltonians predicts higher energies in the extreme populations [Figs. 7(c) and 7(d)]. Clearly, the r -parameter impacts the morphology of the H-surface and then of the phase-space orbits.

IV. DISCUSSION AND CONCLUSION

A comparative analysis of the standard LV model and the GM predator-prey dynamics recently introduced in Ref. 23 has been performed. The GM model is integrable and its closed-form solution assumes an analytical expression involving standard trigonometric cyclic functions. The expression of the oscillation frequency is obtained and only depends on the interaction coefficients, i.e., $\omega = \sqrt{c_{12} c_{21}}$. These results are related to the particular forms of the demographic (natality and mortality) rates and the interaction between the predator and prey populations. For the comparison, the solution of the LV model has been obtained by adopting the standard numerical integration techniques available in the literature. It is shown that the GM model and the LV one exhibit the same main features despite being based on different dynamics.

In order to get further insight into the results of the numerical simulations and their relation to the microstructure of the two set of equations, a few remarks might be conveniently derived from the scaled variables Eqs. (2a) and (8a). The ratio between the scaled amplitudes is the same for the LV and GM model,

$$\frac{X_1}{X_2} = \frac{c_{21} x_1}{c_{12} x_2}. \tag{22}$$

Conversely, the characteristic times exhibit different dependence on the parameters c_{ij} ,

$$T_{GM} = \sqrt{c_{12} c_{21}} t \quad \text{and} \quad T_{LV} = c_{11} t. \tag{23}$$

While T_{LV} simply depends on the predator mortality, the natural time T_{GM} depends on the joint effect of the growth rate of the predator population and the death rate of the prey population, respectively. In other words, the delay between the oscillation phases for the GM model is determined by two parameters related to two

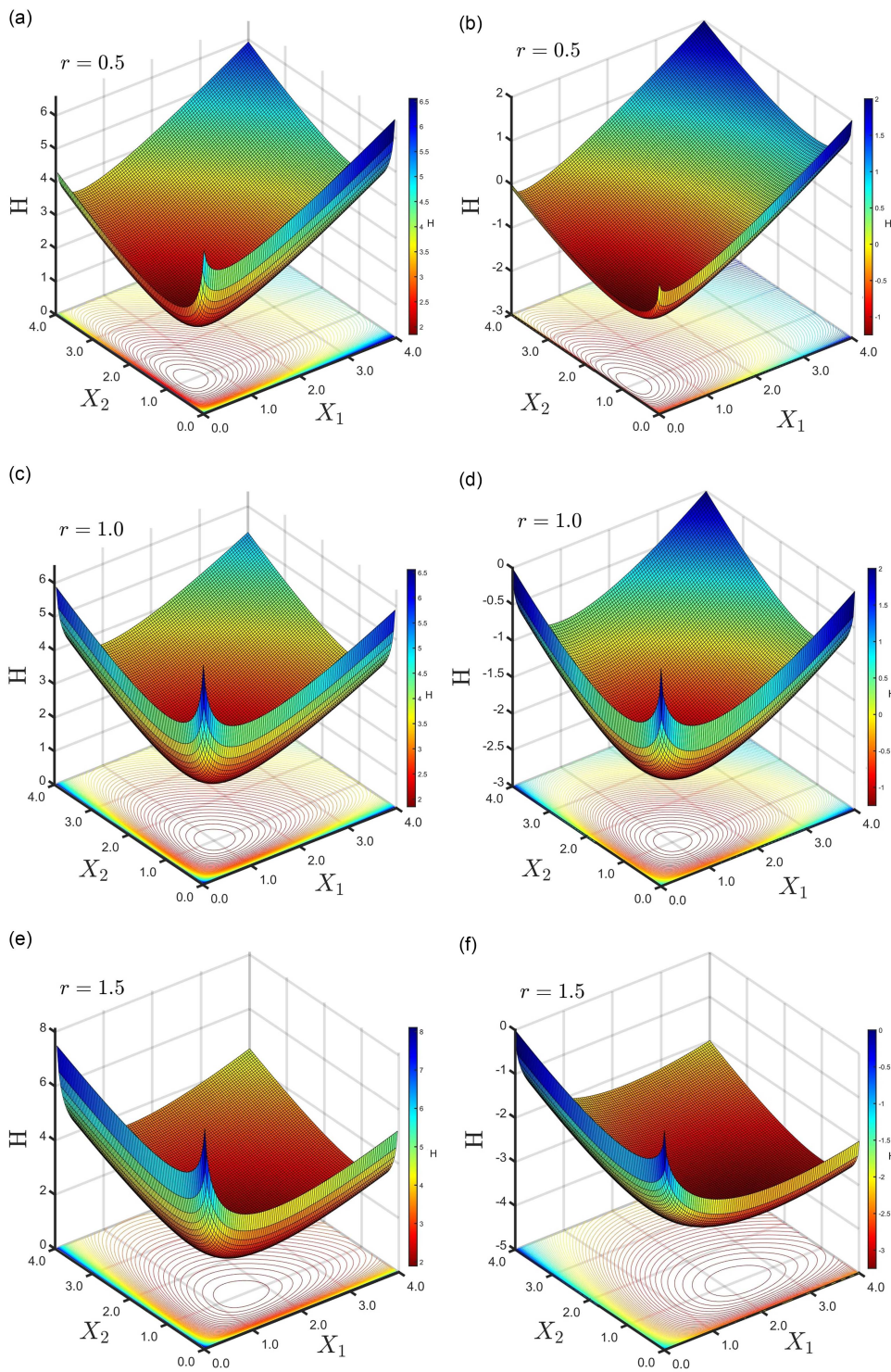


FIG. 7. Contour plot under surface basemap representing the two models' Hamiltonian from a three-dimensional perspective for (a) and (b) $r = 0.5$, (c) and (d) $r = 1.0$, and (e) and (f) $r = 1.5$. The left column refers to the standard LV model described by Eq. (4), while the right one refers to the geometric mean (GM) predator-prey model described by Eq. (9).

populations. Hence, it is characterized by a higher degree of complexity compared to the standard LV model. This difference is also exhibited in the parameter r that in the case of the standard LV model depends only on the demographic parameters. Contrarily, for the GM model, r depends on the interaction strength through c_{12} and c_{21} ,

$$r_{GM} = \frac{c_{22}}{c_{11}} \sqrt{\frac{c_{12}}{c_{21}}} \quad \text{and} \quad r_{LV} = \frac{c_{22}}{c_{11}}, \quad (24)$$

which are equal only in the case of equal interaction rates for the growth and death of the predators and prey. In summary, the interaction parameters rule the temporal scale of the GM model rather than the demographic parameters as in the LV model.

To the purpose of better understanding the mechanism underlying the LV dynamics, it can be observed that the LV model foresees two types of growth and decrease for each population. The rates of decrease of predators and growth of preys depend linearly on the two populations involved. Conversely, the growth rate of predators and the rate of decrease of prey are non-linear functions that depend on the product of the two populations. When only the two linear rates are present in the dynamics, they induce an exponential decrease for the predators and an exponential growth for the preys in the system. In Ref. 41, a limiting case was considered with only the non-linear interaction between the two populations, and it was demonstrated that the dynamics of the system is subject to a saturation of the two populations described by the logistic equation. The predators grow and the preys decrease, asymptotically reaching their limit values. It can, therefore, be concluded that the LV dynamics turns out to be a combination of a linear and a logistic dynamics. The combination of the two integrable dynamics generates the non-integrable LV dynamics. This type of analysis can also be applied to the GM model²³ to better understand its underlying dynamics.

Let us first consider the effects of the demographic dynamics of the system, i.e., the predator mortality and prey birth rate described by the equations $dX_i/dt = -(-r)^{i-1} \sqrt{X_i}$ with $i = 1$ for predators and $i = 2$ for preys. The two equations are decoupled and after their integration, we get

$$X_1(t) = \left(\sqrt{X_{10}} - \frac{1}{2}t \right)^2 \quad \text{and} \quad X_2(t) = \left(\sqrt{X_{20}} + \frac{1}{2}rt \right)^2. \quad (25)$$

The first difference between the GM and LV models is that these equations are quadratic and no longer linear.

A second difference is that while in the LV model, the duration of the phenomenon is infinite; in the GM model, the number of predators decreases non-linearly and the dynamical process evolves within a finite time $0 \leq t \leq 2\sqrt{X_{10}}$, i.e., when their number becomes zero due to their mortality. The preys instead continue to grow with a law that asymptotically becomes linear instead of exponential as in the case of the LV model.

Let us now consider the effects of the predation dynamics, i.e., the predator growth and prey decrease following the interaction between the two populations. The population evolution equations read $dX_i/dt = (-1)^{i-1} \sqrt{X_1 X_2}$, where $i = 1$ corresponds to predators and $i = 2$ to preys. The above system of coupled equations can

be integrated easily obtaining

$$\begin{aligned} X_1(t) &= (X_{10} + X_{20}) \sin^2 \left(a_0 + \frac{1}{2}t \right) \quad \text{and} \\ X_2(t) &= (X_{10} + X_{20}) \cos^2 \left(a_0 + \frac{1}{2}t \right), \end{aligned} \quad (26)$$

with $a_0 = \arcsin \sqrt{X_{10}/(X_{10} + X_{20})}$. The evolution of the system is no longer described by the logistic equation, as in the LV model. An important difference between the two models consists in the fact that while in the LV model, the dynamics has an infinite duration; in the GM model, it ends in a finite time i.e., $0 \leq t \leq t_f$, with $t_f = \frac{\pi}{2} - a_0 > 0$, which corresponds to the instant that the number of preys becomes zero due to predation.

As in the LV model, the overall dynamics of the GM model combines two partial dynamics. The first is the demographic dynamics that accounts for the mortality of predators and the birth rate of preys, while the second dynamics describes the phenomenon of predation accounting for the increase of predators and decrease of preys following the interaction between the two populations. The above partial dynamics are completely different in the two models considered here. The overall dynamics of both models result to be oscillating even if different in the two cases.

ACKNOWLEDGMENTS

This work received financial support from the TED4LAT project within the WIDERA initiative of the Horizon Europe Programme, Grant Agreement No. 101079206.

AUTHOR DECLARATIONS

Conflict of Interest

The authors have no conflicts to disclose.

Author Contributions

S. L. da Silva: Conceptualization (equal); Formal analysis (equal); Investigation (equal); Methodology (equal); Software (equal); Validation (equal); Visualization (equal); Writing – original draft (equal). **A. Carbone:** Conceptualization (equal); Formal analysis (equal); Funding acquisition (equal); Investigation (equal); Methodology (equal); Project administration (equal); Supervision (equal); Validation (equal); Visualization (equal); Writing – original draft (equal). **G. Kaniadakis:** Conceptualization (equal); Formal analysis (equal); Funding acquisition (equal); Investigation (equal); Methodology (equal); Project administration (equal); Supervision (equal); Validation (equal); Visualization (equal); Writing – original draft (equal).

DATA AVAILABILITY

Data sharing is not applicable to this article as no new data were created or analyzed in this study.

REFERENCES

¹A. J. Lotka, *Elements of Physical Biology* (Lippincott Williams and Wilkins, Philadelphia, PA, 1925).

- ²V. Volterra, “Variazioni e fluttuazioni del numero d’individui in specie animali conviventi,” *Memoria della Reale Accademia Nazionale dei Lincei* **2**, 31–113 (1926).
- ³N. S. Goel, S. C. Maitra, and E. W. Montroll, “On the Volterra and other nonlinear models of interacting populations,” *Rev. Mod. Phys.* **43**, 231–276 (1971).
- ⁴M. Peschel and W. Mende, *The Predator-Prey Model. Do We Live in a Volterra World?* (Springer-Verlag, Wien, 1986).
- ⁵T. Ráz, “The Volterra principle generalized,” *Philos. Sci.* **84**, 737–760 (2017).
- ⁶T. Arnoux de Pirey and G. Bunin, “Aging by near-extinctions in many-variable interacting populations,” *Phys. Rev. Lett.* **130**, 098401 (2023).
- ⁷S. Pigolotti, C. López, and E. Hernández-García, “Species clustering in competitive Lotka-Volterra models,” *Phys. Rev. Lett.* **98**, 258101 (2007).
- ⁸J. Bragard, G. Vidal, H. Mancini, C. Mendoza, and S. Boccaletti, “Chaos suppression through asymmetric coupling,” *Chaos* **17**, 043107 (2007).
- ⁹T. M. R. Filho, I. M. Gléria, A. Figueiredo, and L. Brenig, “The Lotka-Volterra canonical format,” *Ecol. Model.* **183**, 95–106 (2005).
- ¹⁰J. Llibre and Y. P. Martínez, “Dynamics of a family of Lotka-Volterra systems in \mathbb{R}^3 ,” *Nonlinear Anal.* **199**, 111915 (2020).
- ¹¹E. K. Waters, H. S. Sidhu, L. A. Sidhu, and G. N. Mercer, “Extended Lotka-Volterra equations incorporating population heterogeneity: Derivation and analysis of the predator-prey case,” *Ecol. Model.* **297**, 187–195 (2015).
- ¹²B. Deng and I. Loladze, “Competitive coexistence in stoichiometric chaos,” *Chaos* **17**, 033108 (2007).
- ¹³A. Ghasemabadi and M. H. Rahmani Doust, “Investigating the dynamics of Lotka-Volterra model with disease in the prey and predator species,” *Int. J. Nonlinear Anal. Appl.* **12**, 633–648 (2021).
- ¹⁴J. Jiang, F. Liang, W. Wu, and S. Huang, “On the first Liapunov coefficient formula of 3D Lotka-Volterra equations with applications to multiplicity of limit cycles,” *J. Differ. Equ.* **284**, 183–218 (2021).
- ¹⁵L. Cairó and M. R. Feix, “Families of invariants of the motion for the Lotka-Volterra equations: The linear polynomials family,” *J. Math. Phys.* **33**, 2440–2455 (1992).
- ¹⁶P. Gatabazi, J. Mba, and E. Pindza, “Fractional gray Lotka-Volterra models with application to cryptocurrencies adoption,” *Chaos* **29**, 073116 (2019).
- ¹⁷W. Cui, R. Marsland, and P. Mehta, “Effect of resource dynamics on species packing in diverse ecosystems,” *Phys. Rev. Lett.* **125**, 048101 (2020).
- ¹⁸M. Leconte, P. Masson, and L. Qi, “Limit cycle oscillations, response time, and the time-dependent solution to the Lotka-Volterra predator-prey model,” *Phys. Plasmas* **29**, 022302 (2022).
- ¹⁹Z.-F. Lin, Y.-M. Liang, J.-L. Zhao, and J.-R. Li, “Predicting solutions of the Lotka-Volterra equation using hybrid deep network,” *Theor. Appl. Mech. Lett.* **12**, 100384 (2022).
- ²⁰M. J. Aschwanden, F. Scholkmann, W. Béthune, W. Schmutz, V. Abramenko, M. C. M. Cheung, D. Müller, A. Benz, G. Chernov, A. G. Kritsuk, J. D. Scargle, A. Melatos, R. V. Wagoner, V. Trimble, and W. H. Green, “Order out of randomness: Self-organization processes in astrophysics,” *Space Sci. Rev.* **214**, 55 (2018).
- ²¹Y. Nutku, “Hamiltonian structure of the Lotka-Volterra equations,” *Phys. Lett. A* **145**, 27–28 (1990).
- ²²C. M. Evans and G. L. Findley, “Analytic solutions to a family of Lotka-Volterra related differential equations,” *J. Math. Chem.* **25**, 181–189 (1999).
- ²³G. Kaniadakis, “Novel predator-prey model admitting exact analytical solution,” *Phys. Rev. E* **106**, 044401 (2022).
- ²⁴M. Bulmer, “Stochastic population models in ecology and epidemiology,” (1961).
- ²⁵R. M. May, “Will a large complex system be stable?,” *Nature* **238**, 413–414 (1972).
- ²⁶B. Spagnolo, A. Fiasconaro, and D. Valenti, “Noise induced phenomena in Lotka-Volterra systems,” *Fluct. Noise Lett.* **3**, L177–L185 (2003).
- ²⁷D. Valenti, A. Fiasconaro, and B. Spagnolo, “Stochastic resonance and noise delayed extinction in a model of two competing species,” *Phys. A: Stat. Mech. Appl.* **331**, 477–486 (2004).
- ²⁸B. Spagnolo, D. Valenti, and A. Fiasconaro, “Noise in ecosystems: A short review,” *arXiv:q-bio/0403004* (2004).
- ²⁹D. Valenti, L. Schimansky-Geier, X. Sailer, and B. Spagnolo, “Moment equations for a spatially extended system of two competing species,” *Eur. Phys. J. B* **50**, 199–203 (2006).
- ³⁰D. Valenti, L. Schimansky-Geier, X. Sailer, B. Spagnolo, and M. Iacomì, “Moment equations in a Lotka-Volterra extended system with time correlated noise,” *Acta Phys. Polonica* **38**(5), 1961–1972 (2006).
- ³¹M. Parker and A. Kamenev, “Extinction in the Lotka-Volterra model,” *Phys. Rev. E* **80**, 021129 (2009).
- ³²P. V. Aceituno, T. Rogers, and H. Schomerus, “Universal hypotrochoidal law for random matrices with cyclic correlations,” *Phys. Rev. E* **100**, 010302 (2019).
- ³³J. W. Baron, T. J. Jewell, C. Ryder, and T. Galla, “Eigenvalues of random matrices with generalized correlations: A path integral approach,” *Phys. Rev. Lett.* **128**, 120601 (2022).
- ³⁴E. Korkmazhan and A. R. Dunn, “High-order correlations in species interactions lead to complex diversity-stability relationships for ecosystems,” *Phys. Rev. E* **105**, 014406 (2022).
- ³⁵P. Mazzetti and A. Carbone, “Periodic and non-periodic brainwaves emerging via stochastic synchronization of closed loops of firing neurons,” *Algorithms* **15**, 396 (2022).
- ³⁶T. Arnoux de Pirey and G. Bunin, “Aging by near-extinctions in many-variable interacting populations,” *Phys. Rev. Lett.* **130**, 098401 (2023).
- ³⁷R. E. Mickens and K. Oyedéji, “A class of generalizations of the Lotka-Volterra predator-prey equations having exactly soluble solutions,” *J. Niger. Math. Soc.* **36**, 47–54 (2017).
- ³⁸P. DeVries and J. Hasbun, *A First Course in Computational Physics* (Jones & Bartlett Learning, 2011).
- ³⁹L. F. Shampine and M. W. Reichelt, “The MATLAB ODE suite,” *SIAM J. Sci. Comput.* **18**, 1–22 (1997).
- ⁴⁰M. S. Laska and J. T. Wootton, “Theoretical concepts and empirical approaches to measuring interaction strength,” *Ecology* **79**, 461–476 (1998).
- ⁴¹J. M. Blanco, “Relationship between the logistic equation and the Lotka-Volterra models,” *Ecol. Model.* **66**, 301–303 (1993).